# Field-free current-induced magnetization switching in GdFeCo: A competition between spin-orbit torques and Oersted fields

Cite as: J. Appl. Phys. **132**, 083903 (2022); doi: 10.1063/5.0091944 Submitted: 23 June 2022 · Accepted: 22 July 2022 · Published Online: 24 August 2022







Jean-Loïs Bello, <sup>1</sup> D Yassine Quessab, <sup>2</sup> D Jun-Wen Xu, <sup>2</sup> D Maxime Vergès, <sup>1</sup> D Héloïse Damas, <sup>1</sup> D Sébastien Petit-Watelot, <sup>1</sup> D Juan-Carlos Rojas Sánchez, <sup>1</sup> D Michel Hehn, <sup>1</sup> D Andrew D. Kent, <sup>2</sup> D and Stéphane Mangin D.

# **AFFILIATIONS**

# **ABSTRACT**

Switching of perpendicular magnetization via spin-orbit torque (SOT) is of particular interest in the development of non-volatile magnetic random access memory (MRAM) devices. We studied current-induced magnetization switching of Ir/GdFeCo/Cu/Pt heterostructures in a Hall cross geometry as a function of the in-plane applied magnetic field. Remarkably, magnetization switching is observed at zero applied field. This is shown to result from the competition between SOT, the Oersted field generated by the charge current, and the material's coercivity. Our results show a means of achieving zero-field switching that can impact the design of future spintronics devices, such as SOT-MRAM.

Published under an exclusive license by AIP Publishing. https://doi.org/10.1063/5.0091944

# INTRODUCTION

The development of magnetic random access memory (MRAM) devices such as spin transfer torque (STT)-MRAM1,2 and spin orbit torque (SOT)-MRAM3-5 depends on advancing the understanding of current-induced magnetization reversal processes. During the past decade, attention has been focused on spin-orbit torque (SOT) switching of perpendicular magnetic anisotropy (PMA) materials to provide a reliable, faster, and scalable platform for SOT-MRAM. Injection of an in-plane charge current in heterostructures generates a transverse spin current due to the structural inversion asymmetry and significant spin-orbit coupling. The resulting out-of-plane spin currents exert a torque, known as the SOT, 6-9 on the magnetization that can switch it. The SOT may have two components, known as the damping-like and field-like torques, which both affect the magnetization of a ferromagnetic (FM) layer in contact with a heavy metal (HM). However, in most studies, SOT switching of perpendicularly magnetized layers is only observed if an in-plane magnetic field is applied that breaks the axial symmetry. For future applications, e.g., low-power memory and computing devices, both low switching current thresholds and operation at zero applied field are required.

Recent research has focused on developing a better understanding of the SOT physics, which can be used to design ultrafast and power efficient spintronic devices. <sup>10–15</sup> To implement field-free SOT devices, different approaches were investigated, such as structural and stack engineering, <sup>16–18</sup> vertical composition gradient, <sup>19</sup> exchange biasing of a FM, <sup>20–24</sup> and the use of ferroelectric substrates. <sup>25</sup> These were explored to realize deterministic external-field-free switching within the SOT device itself.

One material of particular interest is the ferrimagnetic alloy GdFeCo. In this material, the moments on the rare-earth (Gd) sublattice are exchange coupled antiferromagnetically to those on the transition-metal (FeCo) sublattice.<sup>26</sup> The net magnetization and coercivity of the GdFeCo alloy can easily be tuned by changing its composition or the temperature.<sup>27</sup> Moreover, GdFeCo has shown very interesting all optical switching properties<sup>28</sup> and current-induced "self-torque."<sup>29</sup> Different studies involving SOT switching of ferrimagnetic alloys have been reported recently and shown to be very energy efficent.<sup>30–35</sup>

In this paper, we study current-induced magnetization switching in a GdFeCo Hall cross. We demonstrate that current-induced switching can be obtained without any in-plane applied field. A

<sup>&</sup>lt;sup>1</sup>Université de Lorraine, CNRS, IJL, F-54000 Nancy, France

<sup>&</sup>lt;sup>2</sup>Center for Quantum Phenomena, Department of Physics, New York University, New York, New York 10003, USA

a)Author to whom correspondence should be addressed: stephane.mangin@univ-lorraine.fr

state diagram is built from the Hall resistance measurements as a function of the injected current and the in-plane field. Our results can be understood by considering the SOT switching and the effect of the Oersted fields that tend to nucleate longitudinal magnetic domains of opposite direction on each side of the wire. The latter becomes dominant when no in-plane field is applied and leads to a partial magnetization reversal.

# **EXPERIMENTAL DETAILS**

The studied heterostructure,  $SiO_2$ //Ta (5 nm)/Ir (5 nm)/ $Gd_{24.3}Fe_{68.1}Co_{7.6}$  (5 nm)/[Cu (5 nm)/Pt(5 nm), was grown by magnetron sputtering and patterned into  $10\,\mu\text{m}$  wide wires to form a

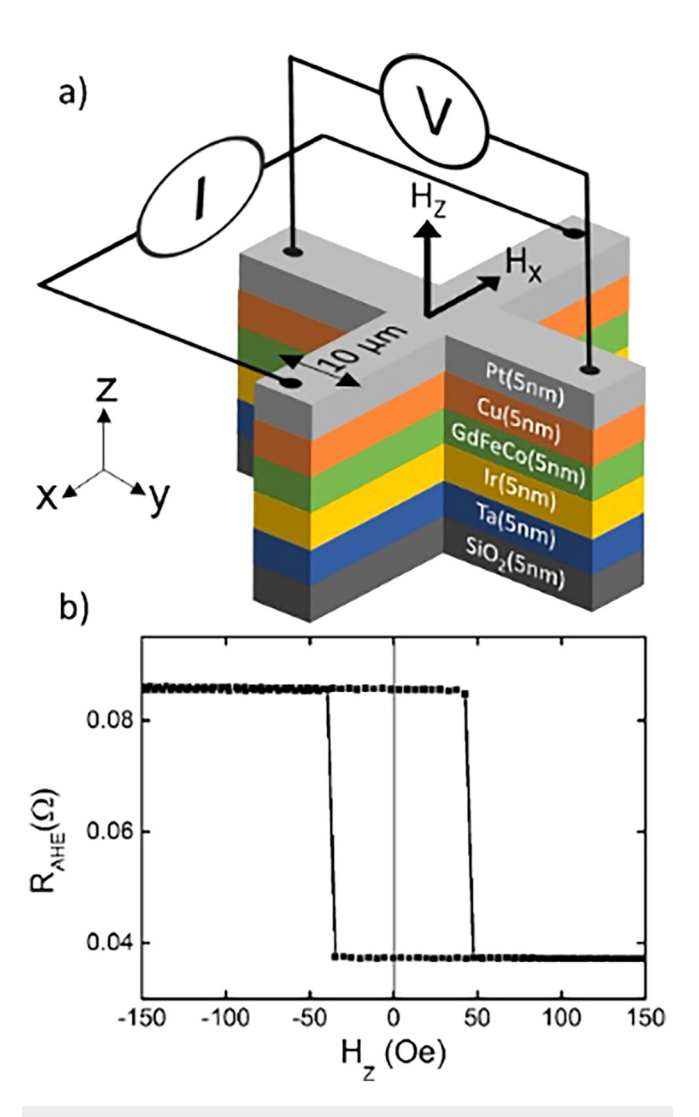


**FIG. 1.** GdFeCo Hall cross: (a) Schematic of the measurement setup and of the GdFeCo sample stack,  $SiO_2$ //Ta (5 nm)/Ir  $(5 \text{ nm})/Gd_{24.3}$ Fe<sub>68.1</sub>Co<sub>7.6</sub> (5 nm)/(Cu (5 nm))/Pt(5 nm). (b) Dependence of the anomalous Hall resistance on the external magnetic field applied perpendicular to the film plane  $H_Z$ .

Hall cross as sketched in Fig. 1. The 5 nm  $Gd_{24.3}Fe_{68.1}Co_{7.6}$  layer is a "FeCo rich" alloy, which means that the alloy's net magnetization is aligned with the FeCo sublattice moments and the compensation temperature is below room temperature. Thus, the net magnetization remains aligned with the FeCo sublattice moments even during current pulses that may heat the sample. The anomalous Hall resistance,  $R_{\rm AHE}$  that is measured as a function of the applied field perpendicular to the film plane, along the z direction, demonstrates that the film has a perpendicular magnetic anisotropy (PMA) [Fig. 1(b)]. This measurement allows us to determine the value of  $R_{\rm AHE}$  when the sample is fully saturated along the positive and the negative z direction.

# **RESULTS AND DISCUSSION**

Current pulses  $100-\mu s$  in duration are injected parallel to the in-plane magnetic field along the x axis. In Fig. 2, we show the Hall resistance measured as a function of the current density and the applied field. Taking into account that the spin Hall angle of Pt is estimated to be 3.5 times larger than that for  $Ir^{36}$  and that the spin

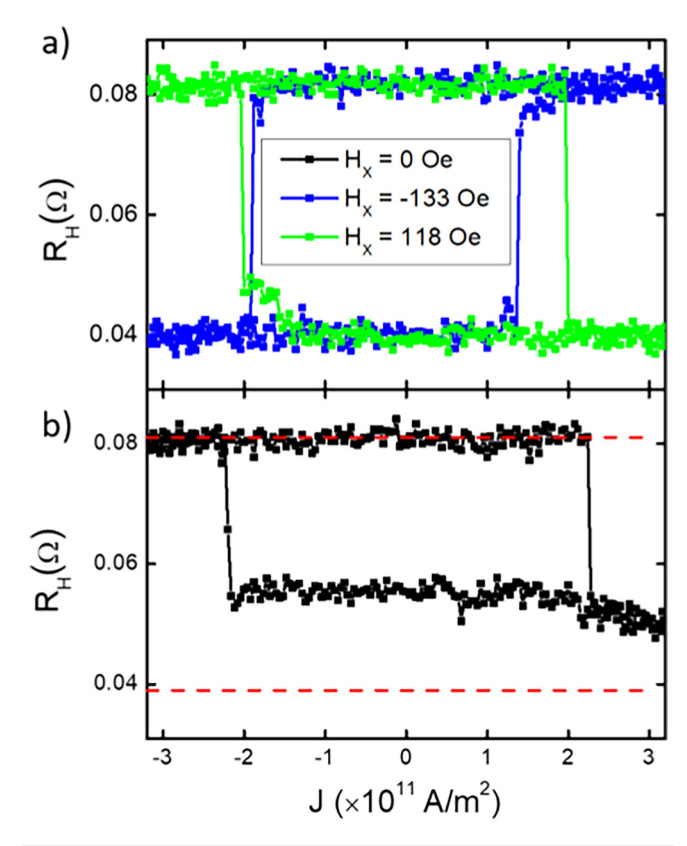


**FIG. 2.** Anomalous Hall resistance measurements on the GdFeCo based device with various in-plane applied fields. (a)  $R_{AHE}$  as a function of the injected current density pulse in two different in-plane applied fields ( $H_x$  = +118 and -133 Oe). (b)  $R_{AHE}$  as a function of the injected current density under no applied field ( $H_x$  = 0).

diffusion length in Cu is much larger than its 5 nm thickness, we concluded that the top Pt layer interfaced with Cu is the main source of spin current leading to SOT. We can observe a full magnetization reversal, i.e., the same amplitude as for  $R_{\rm AHE}$  ( $H_{\rm Z}$ ), with only a small in-plane applied field [Fig. 2(a)]. Note that by changing the sign of the applied field, the symmetry of the hysteresis loop is changed as expected and demonstrated in various SOT studies. Algorithms The current density needed for the switching,  $2 \times 10^{11} \ {\rm A/m^2}$ , is typical of the results reported in the literature. Remarkably, a clear switching is also observed without the applied external field, though the full AHE amplitude is not reached [Fig. 2(b)]. Several reports claiming zero-field switching only show relative AHE amplitudes. Lower AHE effect amplitudes may be attributed to heat effects. However, with a small in-plane applied field, we find that the full AHE amplitude is recovered.

To study in more detail the influence of both the injected current and the in-plane applied field  $(H_x)$ , we created an  $H_x$  current density J  $(H_x$ –J) state diagram, as shown in Fig. 3. For a given in-plane applied field,  $R_{AHE}$  measured while sweeping the current from  $+3\times10^{11}$  to  $-3\times10^{11}$  A/m² was subtracted from the  $R_{AHE}$  value measured while sweeping the current from  $-3\times10^{11}$  to  $+3\times10^{11}$  A/m² to obtain  $\Delta R$ .  $\Delta R$  is different from zero when there is hysteresis. This state diagram allows one to rapidly determine the critical current for switching as a function of the in-plane applied field as well as the AHE amplitude associated with the switching.

The anomalous Hall resistance depends on the projection of the magnetization along z ( $M_Z$ ). Consequently, the in-plane applied field ( $H_x$ ) tilts the magnetization thus reducing the projection on z and as a result  $\Delta R$ . To investigate the mechanism of the current-induced magnetization switching in GdFeCo heterostructures, we combined anomalous Hall resistance measurements with quasistatic Kerr effect microscopy imaging to establish the magnetic state after injecting a current pulse. The magnetic configuration of the GdFeCo Hall cross is shown in Fig. 4 for different current pulse amplitudes. Dark (bright) contrast indicates a

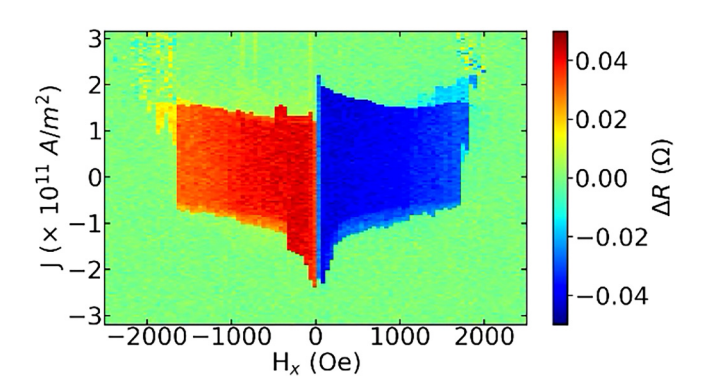


**FIG. 3.** Current density vs in-plane field state diagram. The diagram is obtained by measuring the Hall resistance as a function of the current density for various in-plane applied fields ( $H_x$ ).  $\Delta R$  represents the resistance difference between the resistance measured by sweeping the current density from  $+3 \times 10^{11}$  to  $-3 \times 10^{11}$  A/m² and the one measured by sweeping back the current density from  $-3 \times 10^{11}$  to  $+3 \times 10^{11}$  A/m².

magnetization-up (down) domain. The signature of the Oersted fields created by the injected current pulses can be observed in Figs. 4(b)-4(d). Indeed, the Oersted fields generated by a current flowing in a wire break the magnetization in two domains of opposite direction along the x direction parallel to the current flow.<sup>38</sup>

In Fig. 4, we concentrate on the evolution of the anomalous Hall resistance and the associated magnetic configuration in zero in-plane field  $(H_x = 0)$  as a function of the current density J. Note that the shape of those hysteresis loops ( $R_{AHE}\ vs\ J$ ) varies with the initial magnetic configuration. In Fig. 4(a), two of the typical hysteresis loops are shown. For both, we started by injecting the highest positive current density pulse amplitude  $(+3 \times 10^{11} \text{ A/m}^2)$ leading to the formation of two parallel elongated domains of opposite magnetization direction due to the Oersted field generated by the injected current as seen in Fig. 4(d). Consequently, approximately half of the magnetization in the Hall cross is switched leading to an intermediate anomalous Hall resistance  $(R_{AHE} = 0.07 \Omega)$ . The domain is stable until a current of opposite sign is injected that will generate an Oersted field high enough to drive the domain out of the cross as show in Fig. 4(c). This allows the Hall resistance to reach a saturated state at a value of  $0.04\,\Omega$ . Note that the Hall cross breaks the "wire" symmetry. Indeed, the Oersted field in the cross is lower because the current density is lower and domain may stay in the branches and be dragged.

For larger injected current, the threshold for which a domain can be nucleated on the other side of the Hall cross is reached. Elongated domains with opposite magnetization direction are then

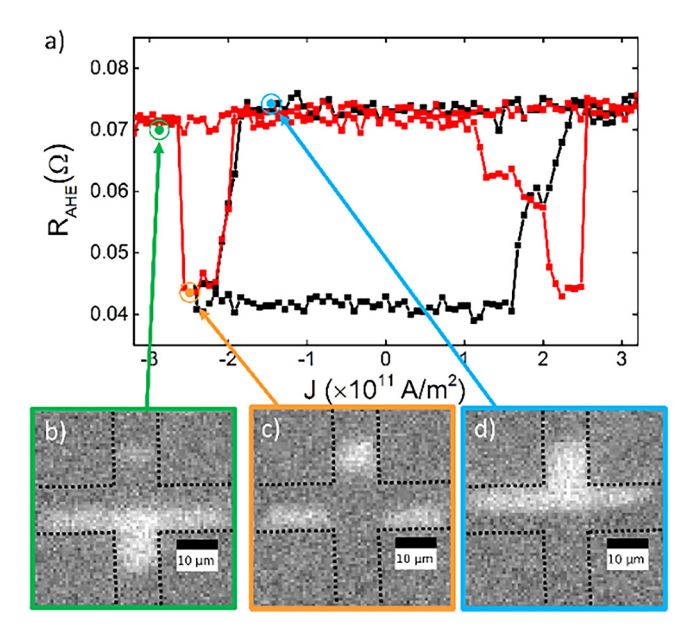


**FIG. 4.** Current-induced magnetization switching under zero applied field in a 10  $\mu$ m Hall cross: (a) Hall resistance R<sub>AHE</sub> as a function of the injected current J starting from large positive current. A full loop in black and a minor loop in red are shown. (b)–(d) are Kerr images taken for different current values as shown in (a).

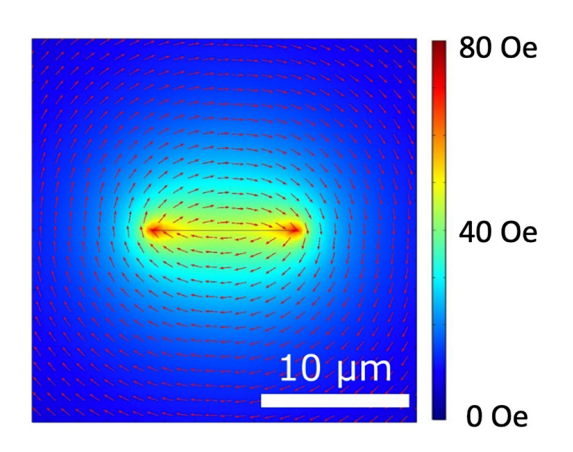


**FIG. 5.** Cross section of the Oersted field obtained using COMSOL® simulations for a current of  $J = 3 \times 10^{11} \text{ A/m}^2$  injected in a Ta(5)/lr(5)/GdFeCo(5)/Cu(5)/Pt(5) 10  $\times$  50  $\times$  25 nm<sup>3</sup> wire.

stabilized as seen in Fig. 4(b), leading to a similar intermediate value for the Hall resistance as in Fig. 4(d). If the injected current is decreased starting from a magnetic configuration shown in Fig. 4(c), a partial square hysteresis loop as shown by the black curve can be obtained [Fig. 4(a)].

In Fig. 5, we show a cross section of the COMSOL® simulation of the generated Oersted field in our stack. First, it confirms that the expected antisymmetric geometry as the magnetic field is perpendicular to the film plane on the edges with opposite directions and in the film plane at the center of the wire. The field reaches 80 Oe, which is more than the coercive field of our sample (50 Oe).

The effects of the Oersted field are often neglected in SOT switching measurements. In our stack, the GdFeCo layer is surrounded by 20 nm of highly conductive metal layers, which can explain its high values for the generated field. Here, we have shown that it strongly affects the reversal of the magnetization by SOT. In Fig. 2, in the presence of an external magnetic field, the loop for  $H_x = -133$  Oe presents a strong asymmetry with respect to the switching current density. This asymmetry follows the path of the Oersted field switching. The Oersted field reduces the SOT threshold current when the switching occurs toward the same state for both mechanisms.

# CONCLUSIONS

In this work, we demonstrated current-induced magnetization switching of GdFeCo heterostructures at zero bias field. Magneto-transport measurements combined with Kerr effect microscopy imaging revealed that the magnetization switching in the GdFeCo Hall crosses is the result of SOTs and the Oersted fields generated by the current pulses. Our findings could help implement field-free SOT based magnetic memories.

# **ACKNOWLEDGMENTS**

This work was supported partly by the French PIA project "Lorraine Université d'Excellence," Reference No. ANR-15-IDEX-04-LUE, by the "SONOMA" and "CapMat" projects co-funded by

"FEDER-FSE Lorraine et Massif Vosges 2014-2020," a European Union Program, and by the Grand Est region and by the Institut Carnot "ICEEL". M.V. is supported by a Cifre PhD grant from Vinci Technologies. The research conducted at NYU was supported under Grant No. NSF-DMR-2105114.

# **AUTHOR DECLARATIONS**

### **Conflict of Interest**

The authors have no conflicts to disclose.

### **Author Contributions**

Jean-Loïs Bello: Formal analysis (equal); Investigation (equal); Methodology (equal). Yassine Quessab: Formal analysis (equal); Investigation (equal); Writing – review & editing (equal). Jun-Wen Xu: Formal analysis (equal); Methodology (equal). Maxime Vergès: Investigation (equal). Héloïse Damas: Investigation (equal). Sébastien Petit-Watelot: Supervision (equal); Validation (equal). Juan-Carlos Rojas Sánchez: Supervision (equal); Validation (equal). Michel Hehn: Supervision (equal); Validation (equal); Writing – review & editing (equal). Andrew D. Kent: Methodology (equal); Supervision (equal); Writing – review & editing (equal). Stéphane Mangin: Conceptualization (equal); Funding acquisition (equal); Methodology (equal); Validation (equal); Writing – original draft (equal).

# **DATA AVAILABILITY**

The data that support the findings of this study are available from the corresponding author upon reasonable request.

# **REFERENCES**

<sup>1</sup>Y. Huai, F. Albert, P. Nguyen, M. Pakala, and T. Valet, Appl. Phys. Lett. 84, 3118 (2004).

<sup>2</sup>M. D. Stiles and A. Zangwill, Phys. Rev. B **66**, 014407 (2002).

<sup>3</sup>M. Cubukcu, O. Boulle, M. Drouard, K. Garello, C. Onur Avci, I. Mihai Miron, J. Langer, B. Ocker, P. Gambardella, and G. Gaudin, Appl. Phys. Lett. **104**, 042406 (2014).

<sup>4</sup>L. Liu, O. J. Lee, T. J. Gudmundsen, D. C. Ralph, and R. A. Buhrman, Phys. Rev. Lett. **109**, 096602 (2012).

<sup>5</sup>J. Ryu, S. Lee, K.-J. Lee, and B.-G. Park, Adv. Mater. 32, 1907148 (2020).

61. M. Miron, K. Garello, G. Gaudin, P.-J. Zermatten, M. V. Costache, S. Auffret, S. Bandiera, B. Rodmacq, A. Schuhl, and P. Gambardella, Nature 476, 189 (2011).

<sup>7</sup>C. Onur Avci, K. Garello, I.-Mihai Miron, G. Gaudin, S. Auffret, O. Boulle, and P. Gambardella, Appl. Phys. Lett. **100**, 212404 (2012).

<sup>8</sup>L. Liu, C.-F. Pai, Y. Li, H. M. Tseng, D. C. Ralph, and R. A. Buhrman, Science 336, 555, (2012).

<sup>9</sup>K. Garello, I. M. Miron, C. O. Avci, F. Freimuth, Y. Mokrousov, S. Blügel, S. Auffret, O. Boulle, G. Gaudin, and P. G. Gambardella, Nat. Nanotechnol. 8, 587 (2013).

<sup>10</sup>K. Cai, Z. Zhu, J. M. Lee, R. Mishra, L. Ren, S. D. Pollard, P. Hen, G. Liang, K. L. Teo, and H. Yang, Nat. Electron. 3, 37 (2020).

<sup>11</sup>K. Jhuria, J. Hohlfeld, A. Pattabi et al., Nat. Electron. 3, 680-686 (2020).

<sup>12</sup>K. S. Lee, S. W. Lee, B. C. Min, and K. J. Lee, Appl. Phys. Lett. **102**, 112410 (2013).

<sup>13</sup>K. Roy, J. Phys. D: Appl. Phys. 47, 422001 (2014).

<sup>14</sup>Q. Hao and G. Xiao, Phys. Rev. Appl. 3, 034009 (2015).

- K. Garello, C. O. Avci, I. M. Miron, M. Baumgartner, A. Ghosh, S. Auffret, O. Boulle, G. Gaudin, and P. Gambardella, Appl. Phys. Lett. 105, 212402 (2014).
   G. Yu, P. Upadhyaya, Y. Fan, J. G. Alzate, W. Jiang, K. L. Wong, S. Takei, S. A. Bender, L.-T. Chang, Y. Jiang, M. Lang, J. Tang, Y. Wang, Y. Tserkovnyak, P. K. Amiri, and K. L. Wang, Nat. Nanotechnol. 9, 548 (2014).
- <sup>17</sup>H. Wu, J. Nance, S. A. Razavi, D. Lujan, B. Dai, Y. Liu, H. He, B. Cui, D. Wu, and K. Wong, Nano Lett. 21, 515–521 (2021).
- <sup>18</sup>A. Kurenkov, C. Zhang, S. DuttaGupta, S. Fukami, and H. Ohno, Appl. Phys. Lett. **110**, 092410 (2017).
- 19Z. Zheng, Y. Zhang, V. Lopez-Dominguez, L. Sánchez-Tejerina, J. Shi, X. Feng, L. Chen, Z. Wang, Z. Zhang, K. Zhang, B. Hong, Y. Xu, Y. Zhang, M. Carpentieri, A. Fert, G. Finnocchio, W. Zhao, and P. Khalili Amiri, Nat. Commun. 12, 4555 (2021).
- <sup>20</sup>Y. W. Oh, S. H. Chris Baek, Y. M. Kim, H. Y. Lee, K. D. Lee, C. G. Yang, E. S. Park, K. S. Lee, K. W. Kim, G. Go, J. R. Jeong, B. C. Min, H. W. Lee, K. J. Lee, and B. G. Park, Nat. Nanotechnol. 11, 878 (2016).
- <sup>21</sup>S. Fukami, C. Zhang, S. DuttaGupta, A. Kurenkov, and H. Ohno, Nat. Mater. 15, 535 (2016).
- <sup>22</sup>A. Kurenkov, C. Zhan, S. DuttaGupta, S. Fukami, and H. Ohno, "Device-size dependence of field-free spin-orbit torque induced magnetization switching in antiferromagnet/ferromagnet structures," Appl. Phys. Lett. 110, 092410 (2017).
- <sup>23</sup>A. van den Brink, G. Vermijs, A. Solignac, J. Koo, J. T. Kohlhepp, H. J. M. Swagten, and B. Koopmans, Nat. Commun. 7, 10854 (2016).
- <sup>24</sup>M. Vergès, V. Kumar, P.-H. Lin, S. Mangin, and C.-H. Lai, AIP Adv. 10, 085320 (2020).
- <sup>25</sup>K. Cai, M. Yang, H. Ju, S. Wang, Y. Ji, B. Li, K. W. Edmonds, Y. Sheng, B. Zhang, N. Zhang, S. Liu, H. Zheng, and K. Wang, Nat. Mater. 16, 712 (2017).
  <sup>26</sup>I. A. Campbell, J. Phys. F: Metal Phys. 2, L47 (1972).
- 27P. Hansen, J. Magn. Magn. Mater. 83, 6 (1990).

- <sup>28</sup>J. Wei, B. Zhang, M. Hehn, W. Zhang, G. Malinowski, Y. Xu, W. Zhao, and S. Mangin, Phys. Rev. Appl. 15, 054065 (2021).
- 29 D. Cespedes-Berrocal, H. Damas, S. Petit-Watelot, D. Maccariello, P. Tang, A. Arriola-Cordova, P. Vallobra, Y. Xu, J. L. Bello, E. Martin, S. Migot, J. Ghanbaja, S. Zhang, M. Hehn, S. Mangin, C. Panagopoulos, V. Cros, A. Fert, and J. C. Rojas-Sanchez, Adv. Mater. 33, 2007047 (2021).
- and J. C. Rojas-Sanchez, Adv. Mater. 33, 2007047 (2021).

  30H. Wu, Y. Xu, P. Deng, Q. Pan, S. A. Razavi, K. Wong, L. Huang, B. Dai, Q. Shao, G. Yu, X. Han, J.-C. Rojas-Sánchez, S. Mangin, and K. L. Wan, Adv. Mater. 31, 1901681 (2019).
- <sup>31</sup>J. Finley and L. Liu, Phys. Rev. Appl. **6**, 054001 (2016).
- <sup>32</sup>Y. Wu, X. Zeng, Y. Guo, Q. Jia, B. Wang, and J. Cao, Appl. Phys. Lett. 118, 022401 (2021).
- <sup>33</sup>T. H. Pham, S.-G. Je, P. Vallobra, T. Fache, D. Lacour, G. Malinowski, M. C. Cyrille, G. Gaudin, O. Boulle, M. Hehn, J.-C. Rojas-Sánchez, and S. Mangin, Phys. Rev. Appl. 9, 064032 (2018).
- <sup>34</sup>R. Mishra, J. Yu, X. Qiu, M. Motapothula, T. Venkatesan, and H. Yang, Phys. Rev. Lett. 118, 167201 (2017).
- 35Y. Quessab, J.-W. Xu, M. G. Morshed, A. W. Ghosh, and A. D. Kent, Adv. Sci. 8, 2100481 (2021).
- 36T. Fache, J.-C. Rojas-Sanchez, L. Badie, S. Mangin, and S. Petit-Watelot, Phys. Rev. B 102, 064425 (2020).
- <sup>37</sup>S.-G. Je, J.-C. Rojas-Sánchez, T. H. Pham, P. Vallobra, G. Malinowski, D. Lacour, T. Fache, M.-C. Cyrille, D.-Y. Kim, S.-B. Choe, M. Belmeguenai, M. Hehn, S. Mangin, G. Gaudin, and O. Boulle, Appl. Phys. Lett. 112, 062401 (2018).
- <sup>38</sup>O. Boulle, L. Heyne, J. Rhensius, M. Kläui, U. Rüdiger, L. Joly, L. Le Guyader, F. Nolting, L. J. Heyderman, G. Malinowski, H. J. M. Swagten, B. Koopmans, C. Ulysse, and G. Faini, J. Appl. Phys. 105, 07C106 (2009).